J. Coat. Technol. Res.
https://doi.org/10.1007/s11998-023-00870-8

The impact of stainless steel flakes as a novel multifunctional pigment for wood coatings

Massimo Calovi, Stefano Rossi

Received: 9 July 2023 / Revised: 8 October 2023 / Accepted: 10 October 2023

Abstract The purpose of this research was to determine the influence of three different amounts of stainless steel flakes on the aesthetic features and durability of a waterborne wood paint. Colorimetric measurements and optical microscope observations were employed to assess the impact of this novel pigment on the overall appearance of the coatings. The effect of the different amounts of metallic flakes on the durability of the layers was evaluated by subjecting the samples to UV-B radiation and cyclic thermal shocks, performing infrared spectroscopy analysis, colorimetric inspections, and adhesion test. In addition, the influence of the filler concentration on the coating barrier efficiency was assessed through the liquid resistance and water uptake tests. Moreover, Buchholz hardness indentation test and the scrub test were conducted to quantify the impact of the flakes on the mechanical characteristics of the coatings, such as hardness and abrasion resistance. Finally, the thermal test evidenced a specific role of the flake amount in altering the thermal behavior of the coatings. Ultimately, this work highlights the attractive effect of stainless steel flakes, which are capable of providing an intense coloring and specific aesthetic features to the paint, preserving the surface's barrier-protective properties, increasing the abrasion resistance of the composite layer, and influencing the thermal behavior of the coating.

Keywords Stainless steel flakes, Wood paint, Protective coating, Layer abrasion resistance, Coating thermal behavior

M. Calovi (✉), S. Rossi
Department of Industrial Engineering, University of Trento, Via Sommarive 9, 38123 Trento, Italy
e-mail: massimo.calovi@unitn.it

Introduction

Wood is a resource that man has learned to exploit and appreciate since ancient times,[1] owing to multiple distinct physical and chemical properties,[2] such as high strength-to-weight ratio[3] and ease of processing.[4] Furthermore, wood is valued for its abundance in nature, as well as for its specific aesthetic qualities.[5,6] Wood is also favorably perceived as a natural and recyclable material, with no CO_2 impact. However, the lignocellulose composition of wood renders this material particularly vulnerable to flames[7,8] and degradation caused by humidity[9,10] and solar radiation.[11–13] To address these practical challenges, wooden surfaces are often covered with organic coatings[14–16] that safeguard the material from solar radiation,[17,18] changes in humidity,[19] chemical attacks,[20] mechanical damage,[21] and the proliferation of damaging microorganisms such as fungi.[22–25]

Because of the increasing demand of wood as material for outdoor implementations, academics and industry have been searching for original ways to improve the functions of wood coatings.[26] The UV protective performance of wood coatings, for instance, has been enhanced through the inclusion of nanoparticles such as TiO_2,[27–29] ZnO,[30,31] SiO_2,[32] and CeO_2.[33,34] Additionally, the high hardness, rigidity, and thermal endurance of nanoparticles such as nanosilica,[35–37] nanoalumina,[38,39] nanoclay,[40,41] and nanocellulose[42,43] have been selected to enhance the physical properties and reduce the water absorption of wood coatings.[44] Ultimately, the addition of nanomaterials such as copper nanopowders,[45] nanotitanium,[46] and silver[47–49] promoted the antibacterial and fungicidal activity of wood paints.

However, the current wood coatings industry is focusing on the application of vibrant color layers,[50] obtained through the exploitation of innovative pigments[51] that impart distinct gloss values to the protec-

Published online: 04 January 2024

tive coatings.[52] In this context, current studies[53–56] investigated the stability of these sources of pigments in wood paints. Indeed, one major challenge in the use of novel pigments is that they must provide distinct aesthetic impacts while preserving the organic coating's protective barrier characteristics. In fact, blending wood paints with a variety of pigments can lead to significant concerns since it may affect the protective features of the organic coating by generating a discontinuity in the polymeric matrix or by proving a low degree of intrinsic stability of the pigment.[57,58]

In this perspective, stainless steel flakes serve as an attractive resource for introducing new aesthetic features and multifunctional properties to wood paints. Recent works have highlighted the excellent contribution of this type of additive in organic matrix composite materials, whose mechanical properties have been enhanced by the stainless steel flakes.[59] Moreover, these fillers have been introduced into organic coatings to improve their protective properties and corrosion resistance performance.[60,61] Similarly, stainless steel flakes proved to be an effective filler for enamel coatings, able to refine the cracking[62] and abrasion resistance[63] of the composite layer. However, the stainless steel flakes possess a further aesthetic function, associated with the specific metallic effect they can impart to the coating, thanks to the particular reflective properties of their structure.[64] Indeed, the current pigment market is strongly oriented toward the application of the so-called high-performance pigments,[65] among which metallic effect pigments are enjoying great success.[66,67] Typically, the metallic appearance in paints is achieved using aluminum-based pigments.[68,69] Nevertheless, stainless steel flakes present a viable substitute due to their increased durability, superior resistance to abrasion, and enhanced aesthetic qualities. Moreover, they exhibit greater stability than aluminum-based substances when exposed into aqueous solutions,[70] rendering them a more effective pigment for water-based paints. Ultimately, stainless steel flakes were originally designed as a pigment to impart a metallic effect, but they have proven to offer additional properties to the coating, going beyond just the visual aspect.

However, despite these premises, stainless steel flakes have never been applied to wood paints. Thus, this study aims to investigate the multifunctional effect of different amounts of stainless steel flakes on the performance of a waterborne paint for wood. The study examines the aesthetic and multifunctional aspects provided by the metallic additive, but examines also the impact of the flakes on the durability of the polymeric coating, in terms of barrier properties, abrasion resistance and thermal behavior.

To determine how the filler concentration effects the distinct characteristics of the coating, three different amounts of flakes were added to a commercial waterborne paint. The aspect of the filler and the appearance of the coatings were analyzed by means of scanning electron microscope (SEM) and optical stereomicroscope observations, as well as with colorimetric analyses, to characterize the effect of the metallic additive on the structure and aesthetic features of the composite layers. The impact of the flakes on the durability of the coatings was evaluated with two distinct accelerated degradation tests, such as the exposure in the climatic chamber and to UV-B radiations, with the aim of assessing the barrier effect and stability/protection with respect to color change, respectively. The possible chemical decay of the coatings owing to UV-B radiation exposures was examined with infrared FTIR measurements, while colorimetric analyses were performed to track any associated aesthetic changes in the coatings. Additionally, colorimetric tests were carried out to examine the risk of coating degradation in the climatic chamber due to the addition of the different amount of flakes. The behavior of the coatings was investigated with visual inspections and observations with the optical microscope, while the cross-cut test was employed to evaluate the effect of the accelerated degradation test on the adhesion of the coatings. Furthermore, the protective performance of the coatings was examined with the chemical resistance test, wettability test, and liquid water uptake test, analyzing probable color changes of the samples, to determine whether the flakes alter the barrier attributes of the paint. Thus, the Buchholz hardness indentation test and the scrub test were used to analyze the effect of the flakes on the mechanical properties of the coatings. Finally, as the flakes appear as dark powders and possess the interesting metallic aesthetic feature, the thermal characteristics of the coating were investigated as a function of the filler concentration, employing a very specific experimental setup.

Materials and methods

Materials

The lamellar stainless steel flakes STAY/STEEL LN 25 were supplied by Eckart Italia (Rivanazzano, Italy) and used as received. The flakes are based on stainless steel AISI 6126 (10.0–20.0 wt.% Cr– < 0.1 wt.% Ni– < 1.0 wt.% Co–2.5–10.0 wt.% Mn–1.0-5.0 wt.% Mb–Fe bal.) and possess a bulk density of 0.2–0.4 g/cm^3. Supplier dimensional analyses specify D10, D50, and D90 values as 3.0–10.0, 20.0–27.0, and 35.0–55.0, respectively. The 150 × 150 × 2 mm^3 poplar wood panels were provided by Cimadom Legnami (Lavis, TN, Italy). The waterborne acrylic bio-based paint TECH20 was supplied by ICA Group (Civitanova Marche, AN, Italy). The paint is made of raw materials from renewable sources. Sodium chloride (≥ 99.0%) and ethanol (99.8%) were purchased from Sigma-Aldrich (St. Louis, MO, USA) and used as received. The commercial detergent disinfectant product Suma Bac D10 Cleaner and Sanitiser (Diversey—Fort Mill, SC, USA), containing benzalkonium chloride (3.0–10.0

wt.%), and the cataphoretic red ink Catafor 502XC (Arsonsisi, Milan, Italy) were purchased and used for the liquid resistance tests.

Sample production

The formulation of the commercial paint was modified by adding three different amounts of the stainless steel flakes, to get a final filler content equal to 0.2 wt.%, 0.5 wt.%, and 1.0 wt.%. Prior to application, the three paint mixtures were mechanically mixed for 30 min. The poplar wood panels were first polished with 320 grit paper to achieve a smooth texture. Thus, the paints were sprayed on the pretreated hardwood surfaces, which were subsequently left to air dry for 4 h at room temperature. The deposition and curing processes were repeated twice. Thus, this work evaluated the effect of different flake amounts in the coatings, as summarized in Table 1, which reveals the nomenclature of the four series of samples involved in the study.

Characterization

The low-vacuum scanning electron microscope SEM JEOL IT 300 (JEOL, Akishima, Tokyo, Japan) and the optical stereomicroscope Nikon SMZ25 (Nikon Instruments Europe, Amstelveen, the Netherlands) were employed to investigate the aspect of the flakes and to explore the morphology of the surface and cross section of the coatings, with the aim of evaluating the impact of the content of flakes on the layers' compactness and structure morphology.

Two accelerated degradation tests simulating the exposure to harsh conditions were performed to stress the coatings, in order to assess any variations in the paint's durability driven on by the application of the flakes.

According to the ASTM G154-16 standard,[71] the samples were placed in a UV-B chamber UV173 Box Co.Fo.Me.Gra (Co.Fo.Me.Gra, Milan, Italy) for 200 h, in order to evaluate the coatings' UV resistance. To determine any possible degradation of the layers, FTIR infrared spectroscopy measurements and colorimetric analyses were carried out. A Varian 4100 FTIR Excalibur spectrometer (Varian, Santa Clara, CA, USA) was used to collect the FTIR spectra in order to look into the chemical alterations of the polymeric matrix. The colorimetric analyses were performed with a Konica Minolta CM-2600d spectrophotometer (Konica Minolta, Tokyo, Japan) with a D65/10° illuminant/observer configuration in SCI mode. The standard mandates the use of intense UV-B radiation, which only partially replicates the samples' exposure to solar radiation. Nonetheless, this specific test was selected precisely to emphasize the potential strengthening impact of the flakes forcing the decay of the samples.

Table 1: Sample nomenclature

Sample nomenclature	Stainless steel flakes (wt.%)
F0.0	0.0
F0.2	0.2
F0.5	0.5
F1.0	1.0

To determine the impact of the fillers on the paint's thermal resistance, extreme heat variations were simulated employing the climatic chamber ACS DM340 (Angelantoni Test Technologies, Perugia, Italy). According to the UNI 9429 standard,[72] the exposure test consisted of 15 cycles made of:

- 4 h at + 50 °C and relative humidity < 30%;
- 4 h at − 20 °C;
- 16 h at room temperature.

To prevent unwanted moisture absorption by the wood substrate, silicone was used to seal the five uncoated surfaces of the 40 × 40 × 2 mm^3 poplar wood samples. Every three cycles of exposure in the climate chamber required the execution of colorimetric investigations to record the changes of the appearance of the coatings throughout the test. Furthermore, optical microscope observations were carried out to examine the emergence of any potential microdefects at the conclusion of the test. Similarly, the cross-cut test was conducted in accordance with ASTM D3359-17 standard,[73] to evaluate potential changes in coating adherence brought on by the alternate thermal cycles.

The chemical resistance test was performed to evaluate the effect of the filler amount on the barrier performance of the acrylic matrix. According to the GB/T 1733-93 standard,[74] filter papers were dipped in 15% sodium chloride solution, 70% ethanol, detergent, and red ink, respectively. The filter papers were then set on the coatings, and a glass cover was placed over it. The glass covers and filter papers were taken off after 24 h, and the liquid that was left on the coatings was absorbed. Colorimetric measurements were conducted to estimate any imprint and discoloration phenomena.

Furthermore, the liquid water uptake test was performed in accordance with the EN 927-5:2007 standard,[75] to determine the water permeability the coatings. To prevent water uptake phenomena by the wooden substrate, the five uncoated surfaces of the 40 × 40 × 2 mm^3 poplar wood panels were entirely sealed with silicone following the procedure carried out for the climatic chamber exposure. The samples were preconditioned at 20 °C and 65% RH before being allowed to float in a water-filled container. The moisture uptake, expressed in g/m^2, was calculated monitoring the mass gain after 6, 24, 48, 72, and 96 h of test.

The impact of the amount of flakes on the mechanical characteristics of the acrylic coatings was investi-

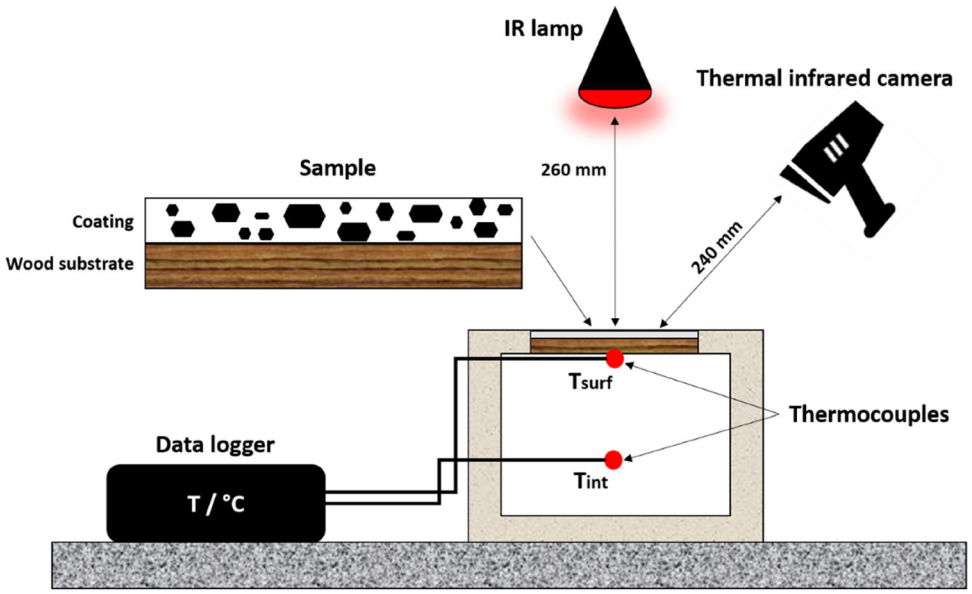

Fig. 1: Experimental setup employed for the thermal behavior measurements performed with the IR emitting lamp

gated using the Buchholz hardness indentation test and the scrub test. The Buchholz test was carried out in accordance with ISO 2815 standard,[76] measuring the length of the indentation induced by the standardized instrument. According to ISO 11998,[77] the scrub test was performed using an Elcometer 1720 Abrasion and Washability Tester (Elcometer, Manchester, UK). Every 250 cycles (37 cycles per minute), for a total of 1000 cycles, the mass loss of the samples was measured to determine the coatings' abrasion resistance. In contrast with the conditions required by the standard, the test was performed without the aid of a cleaning solution in dry mode to avoid the test solution being absorbed into the wood, which would have caused a distortion of the results. Finally, low-vacuum scanning electron microscopy observations were employed to examine the morphology of the damage produced on by the abrasive process on the coatings.

Lastly, the samples were studied with the experimental apparatus shown in Fig. 1**,** already optimized in other works,[78–80] to evaluate the impact of the flakes on the thermal behavior of the paint. The roofless box ($150 \times 270 \times 200$ mm^3) composed of polyurethane foam sheets was covered with the $150 \times 150 \times 2$ mm^3 coated wood samples. A 150-W incandescent infrared emitting lamp (Philips IR150R R125, Eindhoven, Netherlands) was positioned 260 mm above each sample. To measure the temperature values, two distinct thermocouples PT 100 (temperature sensors) were used: one was placed on the back of the coating panel to assess the panel temperature T_{surf} and the other was placed in the center of the box, 100 mm from the coated panel, to measure the small-scale house internal temperature T_{int}. The thermocouples were coupled to a Delta OHM HD 32.7 RTD data recording apparatus (Delta OHM, Caselle di Selvazzano, Italy) for temperature data, which were recorded every 10 s. The instrument was managed by DeltaLog 9 software. The temperature values measured by the thermocouples were recorded until a plateau was reached. Moreover, the external surface temperature of the panels was monitored employing an IR camera FLIR T62101 (FLIR, Milan, Italy). At the conclusion of the test, IR images were captured 240 mm in front of the house model setup, approximately in correspondence of the thermocouple location on the rear part of the panel. Each sample's emittance was taken to be 0.95.

Results and discussion

Flakes and coatings morphology

Figure 2 reveals the morphology of the flakes, observed with the SEM. The flakes appear irregular in shape, with a purely two-dimensional structure. Indeed, the filler consists of sheets with a thickness of less than 1 μm. The width of the sheets, less than 60 μm, allows the flakes to be used as filler in organic coatings with low thicknesses, such as those applied to wooden components.

In this perspective, the four sets of samples were observed in cross section, as shown in the images on the left in Fig. 3, to investigate the distribution and orientation of the flakes within the acrylic layer. Conversely, the images on the right, acquired with the optical microscope, highlight the spatial distribution of the filler, which involves a substantial modification of the appearance of the sample. The addition of the flakes in the paint formulation does not influence the deposition of the coatings, as the four series of layers show comparable thickness, varying between

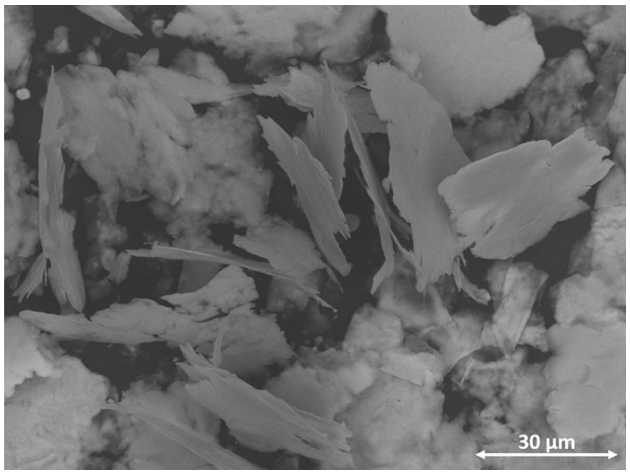

Fig. 2: SEM micrographs of the stainless steel flakes

65 and 80 µm, depending on the irregularity of the surface of the wooden substrate. The spray deposition process results in a random orientation of the flakes within the coating; however, the filler tends to redistribute horizontally during the curing and relaxation process of the acrylic matrix. However, this occurrence does not introduce defects in the coating, which appears free of bubbles or voids at the polymer–flake interface. Consequently, the filler does not significantly affect the coating's structural integrity, whose compactness is preserved. Furthermore, the flakes avoid agglomeration processes, unlike other fillers introduced into polymeric matrices;[81,82] this aspect further limits the possible development of defects in the coating as a consequence of the introduction of the stainless steel-based fillers. Otherwise, the phenomenon of partial orientation of the flakes leads to a substantial change in the appearance of the coating. The top-view images (on the right in Fig. 3) highlight a strong coloring power of the flakes, which lead to a darkening of the composite layer, the intensity of which increases with the amount of filler. The absence of agglomeration phenomena and the homogeneous distribution of the flakes result in a uniform coloring of the coating, suggesting the functional application of these flakes as a pigment for wood paints. Furthermore, the flakes exhibit a metallic effect, which involves an increase in the reflection of light by the coating, as evidenced mainly by the top views in Figs. 3c and 3d, representative of the two samples with the greatest amount of filler.

Figure 4 shows the total color variation of the samples, ΔE, compared to sample F0.0, free of flakes, taken as reference. ΔE has been calculated according to the ASTM E308-18 standard:[83]

$$\Delta E = \left[(\Delta L^*)^2 + (\Delta a^*)^2 + (\Delta b^*)^2\right]^{1/2}$$

where L*, a*, and b* are the colorimetric coordinates for lightness (0 for black and 100 for white objects), the red–green coordinate (positive values are red and negative values are green), and the yellow–blue coordinate (positive values are yellow and negative values are blue), respectively. The graph emphasizes the excellent coloring efficiency of the stainless steel flakes, considering that the literature describes a value of $\Delta E \geq 1$ as being sufficient to be recognized also by the human eye.[84,85] 0.2 wt.% of flakes is sufficient to produce a color change in the coating of approximately 16 points. This phenomenon is caused by a clear reduction of the value of L* (associated with an evident darkening of the layer) and corresponding relative decrease of b* (toward blue tone). Increasing the amount of flakes to 0.5 wt.% results in a color change of approximately 28 points. The further addition of flakes (1.0 wt.%) produces a less evident modification of the appearance, since macroscopically the coating already looks particularly dark.

Thus, these analyses reveal the superior coloring power of the stainless steel flakes, which supply the paint with a distinctive metallic gray color, increasing also the reflectivity of the coating. The functional pigment does not influence the structural morphology of the coating and does not represent a source of particular defects. Definitely, the stainless steel additive can be employed to radically affect the appearance of the coating, changing both its color and reflective properties, providing new aesthetic features to wood paints.

Durability of the coatings in aggressive environments

The stainless steel flakes perform a very distinct function in modifying the appearance of wood paint. Nonetheless, it is crucial to determine whether these additives have an impact on the durability of the paint. Thus, in order to evaluate the effects of various amounts of flakes, the four series of samples were subjected to accelerated degradation tests, including exposure to UV-B radiation and drastic temperature variations.

UV-B exposure

Figure 5 displays the FTIR spectra of the four samples prior to and following the exposure of 200 h in the UV chamber. Their behavior is compared with the wood panel outcome. The latter reveals equivalent peaks in both spectra. The stretching vibration of the –OH group is represented by the region between 3400 cm^{-1} and 3300 cm^{-1},[86] while the –CH group of cellulose, hemicellulose, and lignin is defined by the stretching band between 3000 cm^{-1} and 2800 cm^{-1}.[87] The unconjugated C=O group's stretching vibrations and particular moieties of the polymeric network found in the

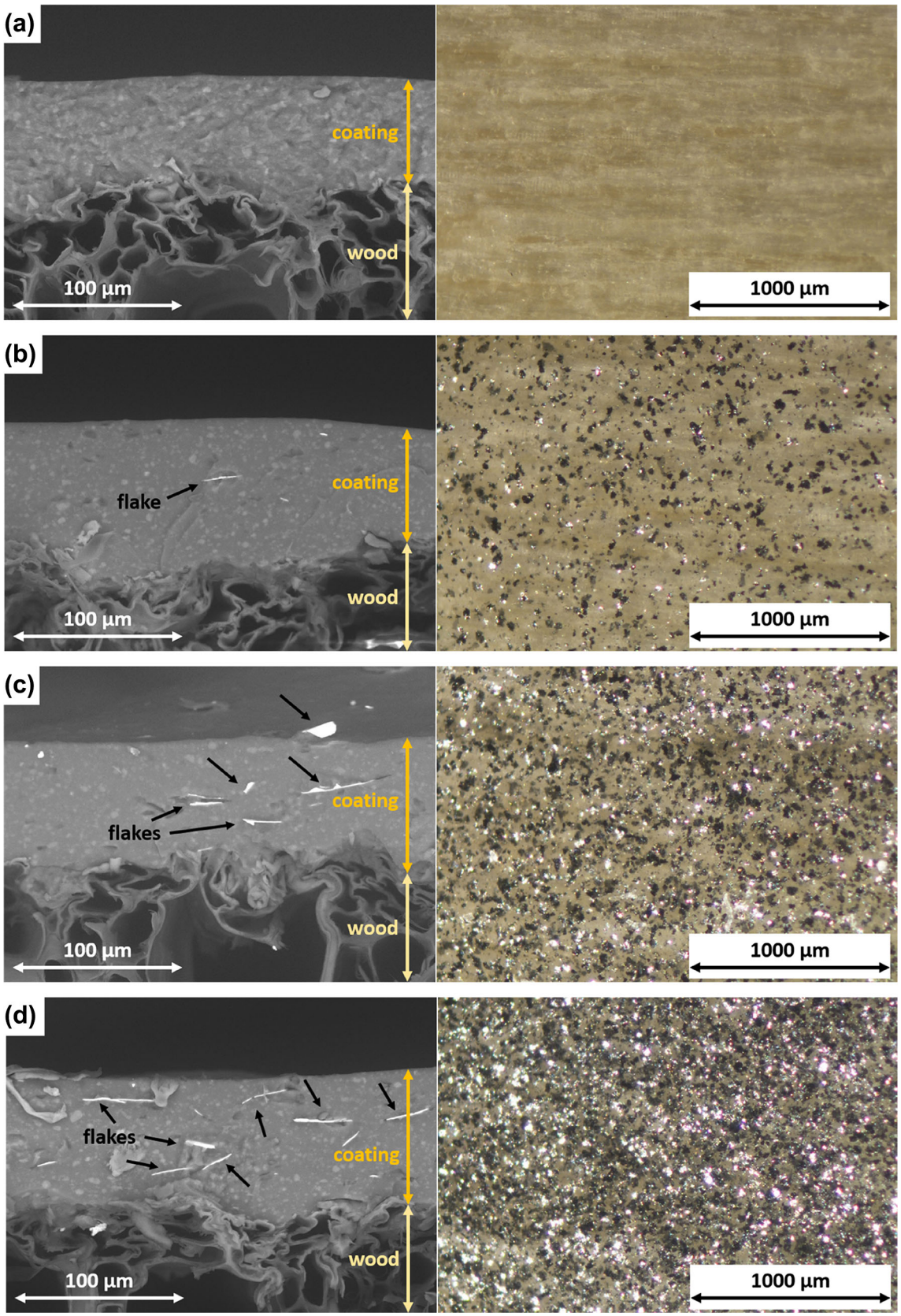

Fig. 3: SEM micrographs of the cross section (on the left) and top-view optical microscope micrographs (on the right) of (a) sample F0.0, (b) sample F0.2, (c) sample F0.5, and (d) sample F1.0

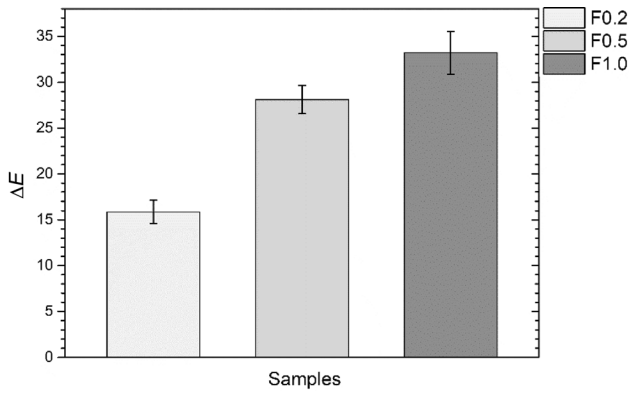

Fig. 4: Color variation of the three coatings containing the flakes compared to sample F0.0

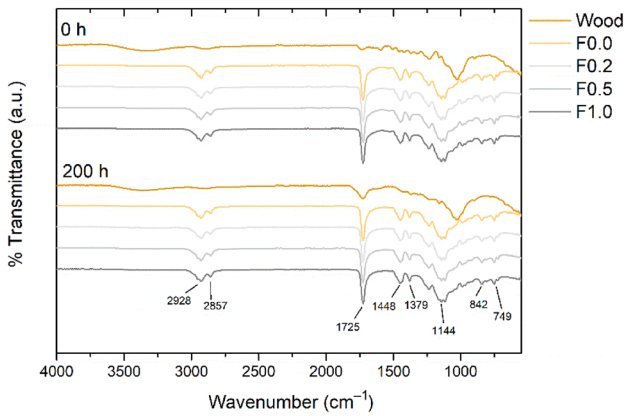

Fig. 5: Evolution of the FTIR spectra of the samples before and after 200 h of exposure to UV-B radiation

wood, like esters, are attributed to the peak at 1726 cm^{-1}.[88] On the other hand, the C=C benzene ring vibration of lignin and the C–H deformation vibration are both represented by the bands at 1590 cm^{-1} and 1462 cm^{-1}, respectively.[89] Finally, the two peaks at 1228 cm^{-1} and 1028 cm^{-1} belong to the C–O stretching and the typical C–O–C stretching vibrations of cellulose,[90] respectively. As a result of the wooden panel exposure to UV-B radiation, the intensity of the peak at 1726 cm^{-1} rises, while the intensity of the peak at 1228 cm^{-1} drops. This result is consistent with the degradation of the wood panel, which is reflected by a modification in the chemical structure of the cellulose.[48]

Otherwise, the FTIR spectra of the four coatings are extremely comparable to each other, with the acrylic paint signal totally masking the peaks of the wooden substrate. Moreover, the presence of the flakes cannot be appreciated by the FTIR measurements. The spectra show two distinct peaks, corresponding to the CH_3 and CH_2 stretching vibrations at 2928 cm^{-1} and 2857 cm^{-1}. The carbonyl stretching band corresponds to the signal with the highest intensity at 1725 cm^{-1}. The two peaks at 1448 cm^{-1} and 1379 cm^{-1} are assumed to be associated to the C–H bending. Likewise, the C–O (ester band) stretching vibration is represented by the broad peak between 1260 cm^{-1} and 960 cm^{-1}. Lastly, the C–H and C–C–C vibrations are reflected by the two signals at 842 cm^{-1} and 749 cm^{-1}, respectively. The spectra of four coatings do not substantially change after the UV-B radiation, suggesting the exceptional resistance of the acrylic paint to UV-induced photo-oxidative decay processes.[91,92]

Figure 6, which illustrates the evolution of the appearance of the samples throughout the accelerated degradation test, reveals that the exposure to UV-B radiation has had a significant impact on their aesthetics even though it was not directly stated by FTIR analysis. The main chemical constituents of poplar wood, cellulose, hemicellulose, and lignin, suffered serious decay. The noticeable yellowing of the wooden panel reflects the outcome of this deterioration process. The sample coated with pure acrylic paint (F0.0) exhibits a similar yellowing process as the wooden panel, even if the extent of the physical–chemical decay of the sample appears to be constrained by the presence of the paint. Actually, acrylic paints exhibit good UV durability,[91,93] and the yellowing of sample F0.0 is caused by the degradation of the underlying wood rather than the chemical deterioration of the coating. This assumption was supported by a recent study,[48] which actually proved that transparent acrylic wood paints do not exhibit aesthetic alterations when applied to surfaces that do not change color when exposed to UV radiation. Therefore, the paint can only partially prevent the phenomena of wood deterioration (as the accelerated degradation test is particularly aggressive). Moreover, due to the paint's transparency, the color change provoked by UV-B radiation in the wooden substrate is not concealed.

On the other hand, the addition of steel flakes seems to hide these decay phenomena. After all, the stability of this material is unaffected by exposure to UV radiation.[94] At the same time, the flakes provide a shielding contribution by partially reflecting the ultraviolet radiation.[95,96] Finally, the flakes have also the advantage of hiding the undesired aesthetic issues caused by the deterioration of the wood, thanks to their strong covering power, similar to other fillers that impart the paint a dark coloring.[80] Indeed, the intensity of the yellowing phenomenon of the sample is considerably reduced by increasing the concentration of flakes, as highlighted in Fig. 6.

This outcome is highlighted by the graph in Fig. 7, which displays the color variation of the samples, monitored during their exposure to UV-B radiation. The chemical–physical decay of the wooden panel occurs rapidly, as evidenced by a strong ΔE, which subsequently settles around 25 points. As previously underlined, the transparent paint is only able to slow down and limit the overall aesthetic modification of the sample induced by UV radiation. Otherwise, the steel flakes substantially reduce this occurrence, even in limited quantities (0.2 wt.%). This result is more

Fig. 6: Change of the appearance of the coated samples and the wooden reference panel during the exposure to UV-B radiation

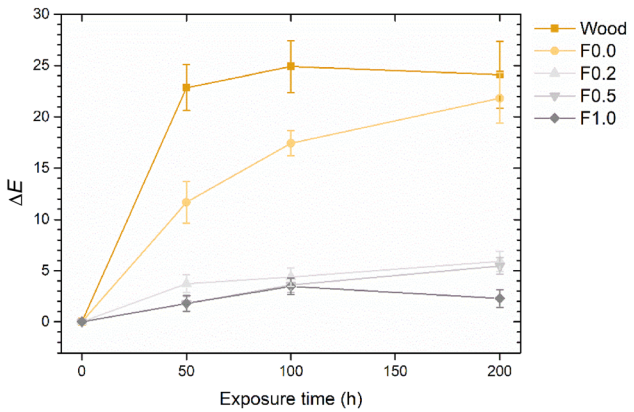

Fig. 7: Color variation of the samples during UV-B exposure

evident by increasing the concentration of filler: the values of ΔE of sample F1.0 are so limited as to be almost negligible.

Finally, the acrylic paint exhibits good chemical resistance to UV-B radiation and is able to modestly slow down the processes of photo-oxidation degradation in the wooden substrate. Nevertheless, the transparency of the paint reveals the yellowing of the wooden substrate. Otherwise, the steel flakes are not susceptible to the accelerated degradation test and are able to partially shield the UV radiation, keeping the aesthetics of the sample almost unchanged. Therefore, the durability and coloring functionality of the pigment are also ensured in outdoor applications, with direct exposure of the painted component to solar radiation.

Climatic chamber exposure

According to criteria displayed in Table 2, the UNI 9429 standard[72] rates the performance of the samples during the climatic chamber exposure test, depending on the development of cracks (defects) and on their possible whitening phenomena.

Because to their fragile behavior at low temperatures and the ease with which moisture can percolate through their inherent bulk porosity, organic coatings typically suffer from abrupt changes in temperature. These events can cause cracks to emerge in the coating,[48,80] which could impair the polymeric layer's capacity to provide adequate protection to the substrate. As a result, the development of cracks is among the most important factors to examine during the assessment of the performance of the coatings subjected to thermal stresses. In this respect, the four sample series displayed successful outcomes, because the corresponding coatings did not reveal obvious cracks. According to the standard, the four layers belong to category 0, as 4× optical microscope observations have not revealed any flaws. Hence, regardless of the quantity of filler added to the coating, it is possible to assert that the flakes do not promote structural deformations of the polymeric matrix resulting from thermal stresses. Moreover, the four samples exhibit a positive behavior also in terms of the stability of their appearance, similar to the ''cracks'' classification. Figure 8 illustrates the evolution of the samples' overall color variation, ΔE, as it was tracked during their exposure in the climatic chamber. The graph is the result of five colorimetric measurements performed for each sample, on five samples per series (total of 25 measurements per series). The samples do not show a specific trend, also influenced by a significant dispersion of the results. However, the values of ΔE are so

Table 2: Categories for whitening and development of cracks following the climatic chamber exposure

Category	Cracks	Whitening
0	No changes	No whitening
1	Fractures visible only with 4× optical system	Light whitening
2	Clearly visible fractures	High whitening

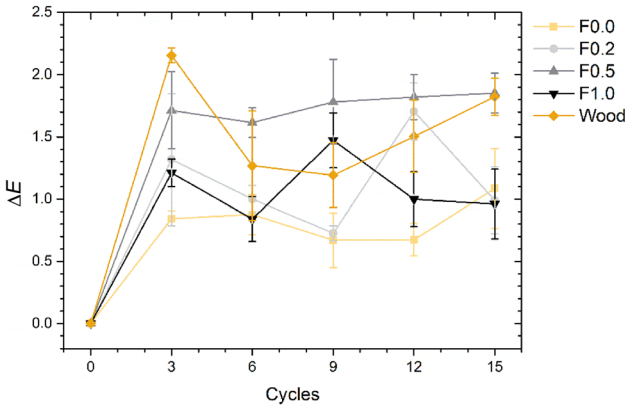

Fig. 8: Color variation of the samples during climatic chamber exposure

negligible that it may be concluded that the accelerated degradation test did not significantly alter the appearance of the coatings. The increase of the value of L* is negligible (less than 1 point), as a symptom of imperceptible whitening phenomena.

Thus, the samples underwent a cross-cut test following the 15 thermal cycles, to determine whether the accelerated degradation test would have triggered adhesion concerns between the coatings and the wooden substrate. The four sample series exhibit adequate adhesion levels even after the numerous heat fluctuations. The outcome of the test is in accordance with level 5B of the ASTM D3359-17 standard,[73] which is representative of any deletion of the layer. Figure 9 depicts the cross-cut test results of sample F0.5, exhibited as an example for all sample series. As a result, the flakes demonstrate that they neither cause noticeable defects in the acrylic matrix nor do they encourage moisture absorption in the coating, preserving the good adhesion of the layer even after repeated thermal stresses.

In conclusion, all of the samples display excellent resistance to persistent temperature variations, with the coatings exhibiting barely detectable whitening phenomena and fracture development. These outcomes are related to the remarkable consistency in adherence of the coatings, which is not compromised by the accelerated degradation test. The addition of stainless steel flakes, which exhibit fascinating durability under thermal stresses, has no consequence on the protective properties of the acrylic paint. Definitely, this kind of additive might function in outdoor coatings that are applied in locations that experience significant temperature variations.

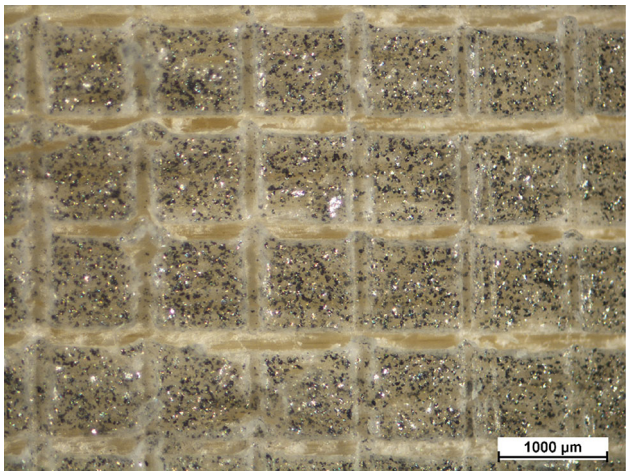

Fig. 9: Cross-cut test results after exposure to the climatic chamber of sample F0.5, observed with optical microscope

Table 3: Color change values corresponding to the level of discoloration

Level	Degree of discoloration	Color difference
0	No color change	≤ 1.5
1	Very slight discoloration	1.6–3.0
2	Slight color change	3.1–6.0
3	Apparent discoloration	6.1–9.0
4	Severe color change	9.1–12.0
5	Complete discoloration	> 12.0

Coatings liquid resistance

The liquid resistance test is usually performed to get valuable data regarding the barrier characteristics of wood coatings and the potential impact of pigments[51,52,80] and additives[43,97] incorporated into the paint. Based on the references in Table 3,[98] the results of the test are evaluated by determining the degree of discoloration induced by the interaction of the coating with the test solutions.

Figure 10 depicts the findings of the analysis, displaying also the specific level of discoloration prompted in the coatings by the four test solutions. The solutions of NaCl, ethanol, and detergent result in a minor alteration of the aspect of the samples, which falls within the level range 0-1. The acrylic paint (sample F0.0) possesses remarkable chemical resistance and seems to be unaffected by the presence of

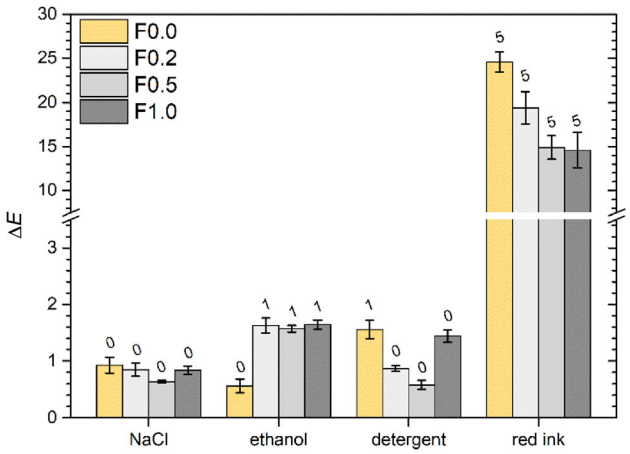

Fig. 10: Color variation of the samples after contact with liquids. The numbers above the columns are representative of the discoloration levels reported in Table 3

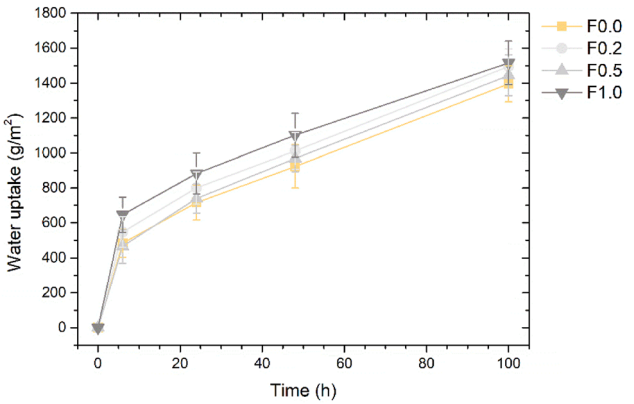

Fig. 11: Evolution of the water uptake during the test

the filler. In fact, the overall ΔE values are so limited as to indicate good insulating features of the composite coatings, even if incorporated with different amounts of stainless steel flakes. However, red ink has a strong impact on the aesthetics of the coatings, causing consistent, grade 5 color changes in the four coatings. This phenomenon was predicted since red ink has an elevated coloring influence and is easily absorbed into the polymeric matrix of paints.[43] Likewise to the outcome of the UV-B radiation exposure test, the dark color of the flakes slightly reduces this color change effect. As a matter of fact, the discoloration imparted by the red ink is less prominent in sample F0.5 and sample F1.0, thanks to the very dark starting shade of the paint.

The test results indicate that the stainless steel flakes have no significant impact on the barrier performance of the acrylic paint, as they do not promote discoloration of the coating when in contact with the four test solutions. The liquid resistance test, on the other hand, yields only qualitative information that is attributed to chromatic changes in the coatings. Thus, the samples were also subjected to the liquid water uptake test, with the aim to evaluate the authentic quantitative implications of the application of the stainless steel flakes on the barrier characteristics of the coatings. Figure 11 represents the progress of the water uptake phenomena recorded during the experiment. The four sets of samples exhibit a similar trend, with significant solution uptake during the first 6 h. Subsequently, the slope of the curves tends to progressively decrease, as the absorption of water by the coatings occurs more slowly. The flakes seem to slightly reduce the barrier contribution of the coating, with water uptake values relatively higher than the corresponding results of sample F0.0. The difference in the outcome of the four samples lies in the rate of absorption during the first 6 h of test: the greater the amount of flakes, the greater the slope of the curves. Typically, the filler introduces discontinuities in the polymeric matrix, which could favor the initial percolation of water inside the layer.[43,99] Although no evident voids were observed at the interface between filler and acrylic matrix, the triggered reduced surface energy enhances the passage of the test solution. However, at the end of the test, the four series of samples show comparable results, highlighting the limited impact of the flakes in compromising the protective performance of the paint.

To summarize, the flakes have no significant effect on the barrier properties of the matrix; however, they can slightly cover the chromatic alterations caused by possible absorption of aggressive solutions. Consequently, also in terms of resistance to liquids, the results support the use of this type of additive as a functional pigment for outdoor applications, in which the coatings can come into contact with external agents.

Coatings hardness and abrasion resistance

The result of the Buchholz hardness test is represented in Fig. 12, where the average length of the indentations generated by the instrument indenting device is attributed to the respective Buchholz hardness value. The outcome of sample F0.2 is comparable with the behavior expressed by the pure acrylic matrix (sample F0.0), as the average length of the indentations in the two coatings are equivalents. The concentration of flakes equal to 0.2 wt.% is so limited that it is unable to provide a significant reinforcing contribution to the polymeric matrix. However, the progressive increase in the amount of filler causes a reduction in the length of the indentations, indicating an increase in the hardness of the composite layers. Sample F0.5 exhibits a high standard deviation, as the distribution and quantity of flakes on the surface of the coating is not sufficient to observe a constant result in terms of surface hardness increase. Otherwise, the distribution of results in the F1.0 sample is much more limited, as the presence of flakes on the surface is so high as to exhibit homoge-

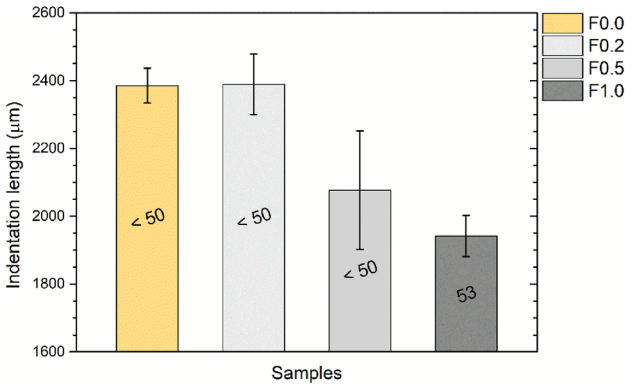

Fig. 12: Evolution of the indentation length of the Buchholz test notches, with the corresponding Buchholz hardness values

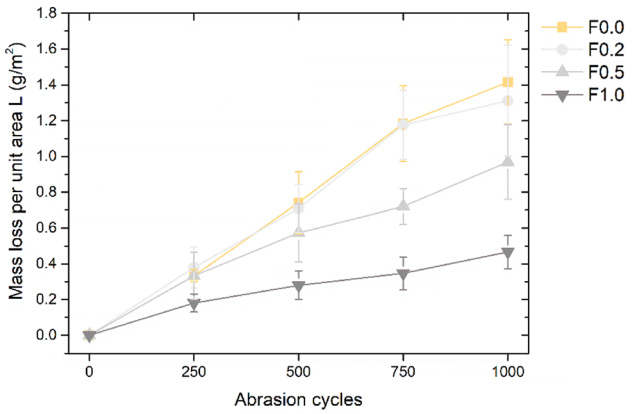

Fig. 13: Coatings mass loss per unit area, as a function of the scrub abrasion cycles number

neous and reproducible results during the test. The average length of the indentations is reduced by 18.6% thanks to the addition of 1 wt.% of flakes. The result is associated with an increase in Buchholz hardness from values < 50 to 53. After all, stainless steel flakes are recognized for their good mechanical properties. A recent study concluded that this type of filler improved the hardness of an aluminum matrix, acting as a hard support element.[100]

The remarkable mechanical properties of the flakes and their good compatibility with the acrylic matrix also have an impact on the abrasion resistance performance of the coating. The trend of the mass loss of the four coatings during the scrub test is depicted in Fig. 13. The removal of material occurs constantly during the test, as evidenced by the almost straight lines of the graph. The behavior of sample F0.2 is fairly similar to that of the reference sample F0.0, as the low amount of flakes does not implement a significant reinforcing characteristic into the acrylic paint, as recognized in the previous hardness test. Conversely, the increase in flake concentration results in a significant reduction in the mass removed by the abrasive processes caused by the scrub test sponge. At the conclusion of the experiment (1000 scrub cycles), samples F0.5 and F1.0 exhibit a mass loss reduction of approximately 31.5% and 67.0%, respectively, compared to the reference sample F0.0. This phenomenon is associated with a substantial rise in the abrasion resistance of coatings loaded with a high quantity of flakes.

To specifically ascertain the strengthening function of the flakes, the samples were examined with SEM at the end of the scrub test. Figure 14 exhibits, as an example, the surface of sample F1.0, revealing both the morphological damage caused by the sponge and the residual presence of the flakes. The horizontal lines are representative of the typical abrasive process developed during the scrub test.[43,81,101] These grooves crafted by the scrub cycles are consistent across the exposed area that came into contact with the abrasive sponge, and run parallel to the pad's movement. The widest grooves are 10 μm wide, denoting that the layers were subjected to vigorous abrasion processes that resulted in significant material removal. Nevertheless, as all of the coatings have thicknesses greater than 65 μm, this degrading phenomenon was not as sufficient as to expose the wooden substrate. The focus in Fig. 14 highlights the presence of the stainless steel flakes (lighter spots), still well anchored to the acrylic matrix. The filler, although subjected to shear stresses resulting from the continuous rubbing of the scrub sponge, appears intact. A recent study investigated the effect of this type of flake on porcelain enamel coatings, revealing the excellent protective performance introduced by the filler, which experienced plastic deformation phenomena due to the abrasive process.[63] Similarly, the filler depicted in the figure has not been removed from the coating, but instead allows for partial protection of the surrounding acrylic matrix, reducing coating mass loss due to abrasion and enhancing the protective features of the composite layer.

In conclusion, the stainless steel flakes provide a functional protective contribution, increasing the overall hardness of the composite layer and reducing the mass loss provoked by abrasion phenomena. This type of additive does not simply perform an aesthetic function as alternative pigment resource, but is also capable of enhancing the mechanical properties of the acrylic matrix without compromising the durability of the coating.

Coatings thermal behavior

Figure 15 depicts the thermal response of the samples considering both the internal temperature T_{int} (dotted lines) and the panel temperature T_{surf}. Regardless of the sample under inspection, the values of T_{surf} reach a sort of plateau around 1200 s after turning on the IR lamps. The specific value of the temperature achieved during the test distinguishes the four categories of samples. In comparison with the reference sample F0.0,

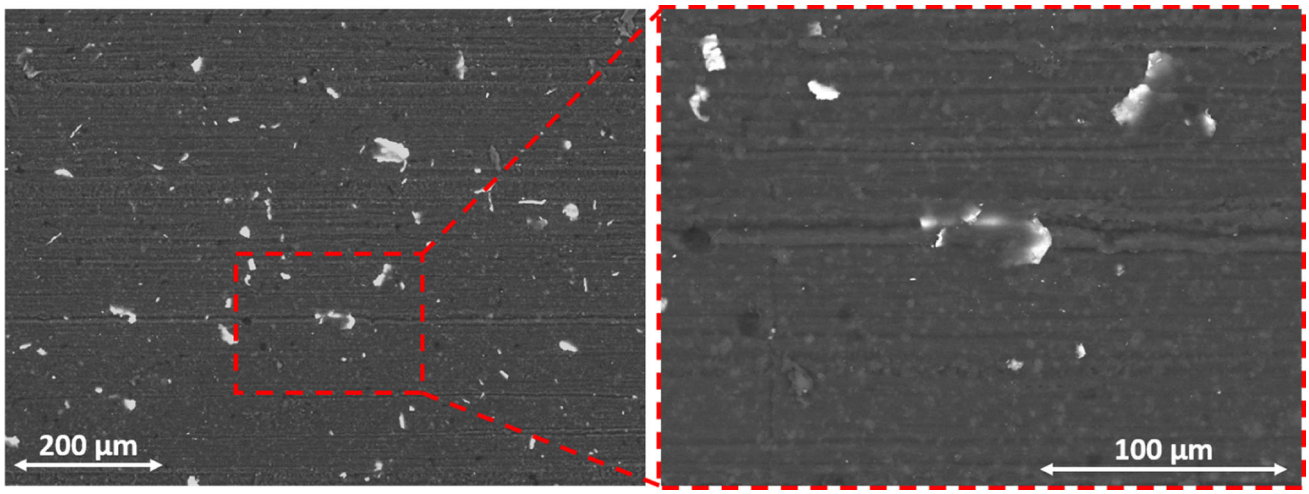

Fig. 14: Top-view SEM micrographs of the surface morphology of sample F1.0 after the 1000 scrub test cycles

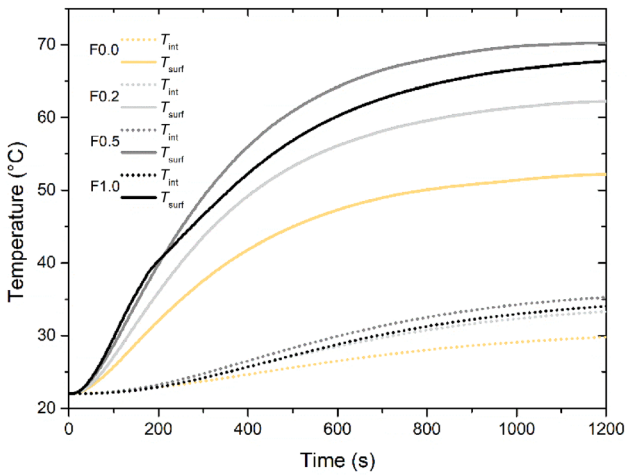

Fig. 15: Coatings thermal behavior

samples F0.2 and F0.5 exhibit an increase in panel temperature of roughly 10.1 °C and 18.1 °C, respectively, at the end of the IR light irradiation test. This occurrence results in a modest increase in indoor temperature T_{int} of roughly 3.5 °C and 5.5 °C, respectively. These measured temperature increases are closely associated with the appearance of the coating, which differs according to the amount of flakes: the greater the filler content, the darker the composite layer becomes, as evidenced by the images in Fig. 3 and the graph in Fig. 4. After all, it has already been amply demonstrated that dark pigments actually lead to an increase in the temperatures of the structures to which they are applied.[77,102–104]

However, a further increase in flakes causes a reduction in temperature values. Doubling the content of the filler from 0.5 wt.% to 1.0 wt.% results in a decrease in T_{int} and T_{surf} of 1.2 °C and 2.5 °C, respectively. This particular phenomenon is due to the reflective characteristics of the metal flakes, which reduce the accumulation of heat in the coating. This episode is well highlighted in the top-view images of Fig. 3, where sample F1.0 significantly reflects the light emitted by the optical microscope. In fact, the T_{surf} curve of sample F1.0 in Fig. 15 undergoes a significant bend around 40 °C, with a consequent reduction in growth speed. The reflective feature of the flakes plays a fundamental role in mitigating the increase in temperature associated to their basically dark shade. As a result, it is possible to assert that the thermal behavior of stainless steel flakes is based on two opposed contributions: the increase in coating darkness causes a raise in absorbed heat, while the improved light reflectance is associated with a decrease in coating temperatures.

To emphasize this aspect, the images in Fig. 16 illustrate the accurate temperature values of the surface exposed to IR radiation as measured by the IR camera at the end of the test. The surface temperature of the panels reaches the maximum peak in sample F0.5, equal to 123.1 °C, and then decreases in sample F1.0, settling at 111.2 °C. Therefore, the trend of T_{surf} corresponds to that of the external temperature of the panels. The light reflectance behavior of the paint is strictly connected to the amount of heat absorbed by the panel and transmitted to the structure.

Ultimately, the quantity of flakes added to the paint can be selected according to the thermal purpose of the paint itself. In order to maximize heat absorption, a limit concentration should not be exceeded so as to reduce the reflecting contribution of the filler. Considering we live in a historical period where the energy and raw resources required to heat an environment are becoming less and less sustainable, the amount of flakes could be optimized in order to preserve energy and avoid material waste. Otherwise, considering the current issues of global warming, the metallic effect of the flakes can be exploited to obtain dark colored coatings, but with a high reflectance, able to mitigate the so-called urban heat island effect (UHI effect). As

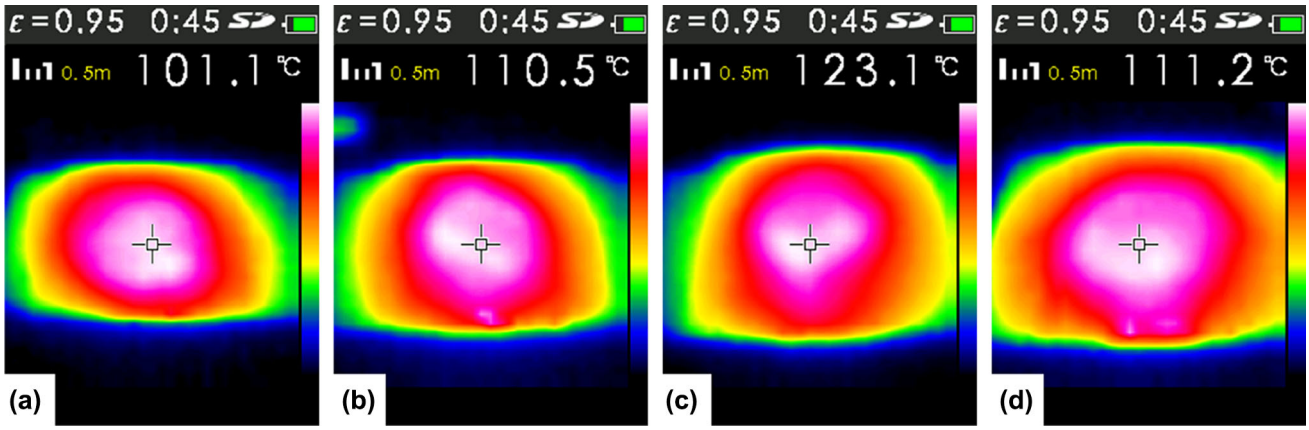

Fig. 16: Infrared images of the external surface temperature of (a) sample F0.0, (b) sample F0.2, (c) sample F0.5, and (d) sample F1.0, acquired with the thermographic camera at the end of the thermal test. The images also show the temperature value measured in the center of the box

a result, the flake content plays a key role in the thermal features of the coating, where it is desired to reduce or enhance the heat absorbed by the structure to which it is applied.

Conclusions

This work investigates the effect of different amounts of stainless steel flakes on the aesthetic and functional features of a wood paint. The analyses reveal the remarkable coloring influence of the filler, which imparts the paint with a specific metallic gray color. The functional pigment has no effect on the structural morphology of the coating and does not constitute a source of particular defectiveness into the polymeric matrix. Thus, the stainless steel addition can be employed to drastically alter the overall look of the coating, modifying both its hue and reflective characteristics, offering wood paints new decorative attributes.

The color change of the coatings caused by UV-B radiation exposure can be mitigated by the flakes, which may partially shield the UV radiation. Furthermore, the stainless steel flakes display remarkable resilience under thermal stress and have no effect on the protective characteristics of the acrylic paint, as well as on the adhesion values of the composite layer. Certainly, this type of filler could be useful in outdoor coatings employed in environment with significant temperature changes and direct exposure to solar radiation.

Moreover, the flakes have no major impact on the barrier characteristics of the matrix; nevertheless, they can partially mask the chromatic shifts induced by potential absorption of solutions. As a result, the findings of the liquid resistance tests justify the application of this type of flake as a functional pigment for outdoor applications where the coatings may interact with external aggressive agents.

The mechanical tests evidenced that the stainless steel flakes additionally offer a functional protective contribution, enhancing the overall hardness of the coatings while decreasing the mass loss caused by abrasion processes. The metallic filler not only serves as an unusual pigment resource, but it can also improve the mechanical characteristics of the acrylic matrix, ensuring the high durability of the composite layer.

Finally, the thermal analyses revealed that the flake amount has a significant impact on the thermal properties of the coating, as the behavior of stainless steel flakes relies on two competing contributions. The enhanced coating darkness leads to a rise in absorbed heat, while the increased light reflectance results in a reduction of coating temperatures. Thus, the filler concentration can be properly selected to minimize or increase the heat absorbed by the substrate to which the coating must be applied.

In conclusion, this study proved that the stainless steel flakes represent an innovative filler for wood coating, as they provide intense coloring and specific aesthetic features to the paint, do not affect the barrier properties of the surface, increase the abrasion resistance of the coating and influence the thermal behavior of the composite layer.

Acknowledgments The authors greatly acknowledge the contributions of Stefano Di Blase (ICA Group, Civitanova Marche, MC, Italy) and Mauro Giuriato (Eckart Italia, Rivanazzano, MI, Italy) regarding the paint and stainless steel flakes supply, respectively. The

publication was created with the co-financing of the European Union—FSE-REACT-EU, PON Research and Innovation 2014-2020 DM1062/2021.

Author contributions MC was involved in conceptualization, methodology, validation, investigation, data curation, and writing—original draft. SR was involved in resources, writing—review and editing, supervision, and project administration.

Funding Open access funding provided by Università degli Studi di Trento within the CRUI-CARE Agreement. The authors did not receive support from any organization for the submitted work.

Conflict of interest The authors have no relevant financial or nonfinancial interests to disclose.

References

1. Radkau, J, *Wood: A History*. Polity Press, Cambridge (2012)
2. Hoadley, RB, ''Chemical and Physical Properties of Wood.'' *The Structural Conservation of Panel Paintings: Proceedings. Part 1: Wood Science and Technology*, 2-20, 1998
3. Hao, J, Wu, X, Oporto, G, Liu, W, Wang, J, ''Structural Analysis and Strength-to-weight Optimization of Wood-based Sandwich Composite with Honeycomb Core Under Three-point Flexural Test.'' *Eur. J. Wood Wood Prod.*, **78** (6) 1195–1207 (2020)
4. Kim, JK, Pal, K, *Recent Advances in the Processing of Wood-plastic Composites*. Springer-Verlag, Berlin Heidelberg (2010)
5. Janin, G, Gonçalez, JC, Ananías, RA, Charrier, B, Silva, GFd, Dilem, A, ''Aesthetics Appreciation of Wood Colour andPatterns by Colorimetry. Part 1. Colorimetry Theory for the CIELab System.'' *Maderas: Cienc. Tecnol.*, **3** (1–2) (2001)
6. Broman, NO, ''Aesthetic Properties in Knotty Wood Surfaces and Their Connection with People's Preferences.'' *J. Wood Sci.*, **47** (3) 192–198 (2001)
7. Lowden, LA, Hull, TR, ''Flammability Behaviour of Wood and a Review of the Methods for Its Reduction.'' *Fire Sci. Rev.*, **2** (1) 1–19 (2013)
8. Stamm, AJ, ''Thermal Degradation of Wood and Cellulose.'' *J. Ind. Eng. Chem.*, **48** (3) 413–417 (1956)
9. Tolvaj, L, Popescu, C-M, Molnar, Z, Preklet, E, ''Effects of Air Relative Humidity and Temperature on Photodegradation Processes in Beech and Spruce Wood.'' *BioResources*, **11** (1) 296–305 (2016)
10. Borrega, M, Kärenlampi, PP, ''Effect of Relative Humidity on Thermal Degradation of Norway Spruce (Picea abies) Wood.'' *J. Wood Sci.*, **54** (4) 323–328 (2008)
11. Mattonai, M, Watanabe, A, Shiono, A, Ribechini, E, ''Degradation of Wood by UV Light: A Study by EGA-MS and Py-GC/MS with On Line Irradiation System.'' *J. Anal. Appl. Pyrolysis*, **139** 224–232 (2019)
12. Hon, DNS, Chang, ST, ''Surface Degradation of Wood by Ultraviolet Light.'' *J. Polym. Sci. Polym. Chem. Ed.*, **22** (9) 2227–2241 (1984)
13. Pandey, KK, ''A Note on the Influence of Extractives on the Photo-discoloration and Photo-degradation of Wood.'' *Polym. Degrad. Stab.*, **87** (2) 375–379 (2005)
14. Pánek, M, Reinprecht, L, ''Colour Stability and Surface Defects of Naturally Aged Wood Treated with Transparent Paints for Exterior Constructions.'' *Wood Res.*, **59** (3) 421–430 (2014)
15. Ahola, P, ''Adhesion Between Paints and Wooden Substrates: Effects of Pre-treatments and Weathering of Wood.'' *Mater. Struct.*, **28** (6) 350–356 (1995)
16. Zareanshahraki, F, Mannari, V, ''Formulation and Optimization of Radiation-Curable Nonisocyanate Polyurethane Wood Coatings by Mixture Experimental Design.'' *J. Coat. Technol. Res.*, **18** (3) 695–715 (2021)
17. Bansal, R, Nair, S, Pandey, KK, ''UV Resistant Wood Coating Based on Zinc Oxide and Cerium Oxide Dispersed Linseed Oil Nano-emulsion.'' *Mater. Today Commun.*, **30** 103177 (2022)
18. Nowaczyk-Organista, M and Oleszek, T, ''Weathering Resistance of Water-borne Wood Coatings Modified with Metal Nano Oxides.'' *Proc. 27th International Conference on Wood Science and Technology, ICWST 2016: Implementation of Wood Science in Woodworking Sector - Proceedings*, 2016
19. Jirouš-Rajković, V, Miklečić, J, ''Enhancing Weathering Resistance of Wood—A Review.'' *Polymers*, **13** (12) 1980 (2021)
20. Hochmańska-Kaniewska, P, Janiszewska, D, Oleszek, T, ''Enhancement of the Properties of Acrylic Wood Coatings with the Use of Biopolymers.'' *Prog. Org. Coat.*, **162** 106522 (2022)
21. Veigel, S, Grüll, G, Pinkl, S, Obersriebnig, M, Müller, U, Gindl-Altmutter, W, ''Improving the Mechanical Resistance of Waterborne Wood Coatings by Adding Cellulose Nanofibres.'' *React. Funct. Polym.*, **85** 214–220 (2014)
22. Šimůnková, K, Hýsek, Š, Reinprecht, L, Šobotník, J, Lišková, T, Pánek, M, ''Lavender Oil as Eco-friendly Alternative to Protect Wood Against Termites Without Negative Effect on Wood Properties.'' *Sci. Rep.*, **12** (1) 1–10 (2022)
23. Miri Tari, SM, Tarmian, A, Azadfallah, M, ''Improving Fungal Decay Resistance of Solvent and Waterborne Polyurethane-Coated Wood by Free and Microencapsulated Thyme Essential Oil.'' *J. Coat. Technol. Res.*, **19** 959–966 (2022)
24. Rosu, L, Varganici, CD, Mustata, F, Rosu, D, Rosca, I, Rusu, T, ''Epoxy Coatings Based on Modified

Vegetable Oils for Wood Surface Protection Against Fungal Degradation.'' *ACS Appl. Mater. Interfaces*, **12** (12) 14443–14458 (2020)
25. Rosu, L, Mustata, F, Varganici, CD, Rosu, D, Rusu, T, Rosca, I, ''Thermal Behaviour and Fungi Resistance of Composites Based on Wood and Natural and Synthetic Epoxy Resins Cured with Maleopimaric Acid.'' *Polym. Degrad. Stab.*, **160** 148–161 (2019)
26. Nikolic, M, Lawther, JM, Sanadi, AR, ''Use of Nanofillers in Wood Coatings: A Scientific Review.'' *J. Coat. Technol. Res.*, **12** (3) 445–461 (2015)
27. Pacheco, CM, Cecilia, BA, Reyes, G, Oviedo, C, Fernández-Pérez, A, Elso, M and Rojas, OJ, ''Nanocomposite Additive of SiO_2/TiO_2/Nanocellulose on Waterborne Coating Formulations for Mechanical and Aesthetic Properties Stability on Wood.'' *Mater. Today Commun*., 29 (2021)
28. Allen, N, Edge, M, Ortega, A, Liauw, C, Stratton, J, McIntyre, R, ''Behaviour of Nanoparticle (Ultrafine) Titanium Dioxide Pigments and Stabilisers on the Photooxidative Stability of Water Based Acrylic and Isocyanate Based Acrylic Coatings.'' *Polym. Degrad. Stab.*, **78** 467–478 (2002)
29. Veronovski, N, Verhovaek, D, Godnjavec, J, ''The Influence of Surface-Treated Nano-TiO_2 (Rutile) Incorporation in Water-Based Acrylic Coatings on Wood Protection.'' *Wood Sci. Technol.*, **47** 317–328 (2012)
30. Salla, J, Pandey, K, Srinivasa, K, ''Improvement of UV Resistance of Wood Surfaces by Using ZnO Nanoparticles.'' *Polym. Degrad. Stab.*, **97** 592–596 (2012)
31. Saha, S, Kocaefe, D, Krause, C, Larouche, T, ''Effect of Titania and Zinc Oxide Particles on Acrylic Polyurethane Coating Performance.'' *Prog. Org. Coat.*, **70** (4) 170–177 (2011)
32. Jalili, MM, Moradian, S, Dastmalchian, H, Karbasi, A, ''Investigating the Variations in Properties of 2-pack Polyurethane Clear Coat Through Separate Incorporation of Hydrophilic and Hydrophobic Nano-silica.'' *Prog. Org. Coat.*, **59** (1) 81–87 (2007)
33. Janesch, J, Czabany, I, Hansmann, C, Mautner, A, Rosenau, T, Gindl-Altmutter, W, ''Transparent Layer-by-Layer Coatings Based on Biopolymers and CeO_2 to Protect Wood From UV Light.'' *Prog. Org. Coat.*, **138** 105409 (2020)
34. Saha, S, Kocaefe, D, Boluk, Y, Pichette, A, ''Surface Degradation of CeO_2 Stabilized Acrylic Polyurethane Coated Thermally Treated Jack Pine During Accelerated Weathering.'' *Appl. Surf. Sci.*, **276** 86–94 (2013)
35. Cheumani Yona, AM, Žigon, J, Ngueteu Kamlo, A, Pavlič, M, Dahle, S, Petrič, M, ''Preparation, Surface Characterization, and Water Resistance of Silicate and Sol-Silicate Inorganic-Organic Hybrid Dispersion Coatings for Wood.'' *Materials*, **14** (13) 3559 (2021)
36. Salleh, NGN, Alias, MS, Gläsel, H, Mehnert, R, ''High Performance Radiation Curable Hybrid Coatings.'' *Radiat. Phys. Chem.*, **84** 70–73 (2013)
37. Zhang, S, Guo, M, Chen, Z, Liu, QH, Liu, X, ''Grafting Photosensitive Polyurethane onto Colloidal Silica for Use in UV-curing Polyurethane Nanocomposites.'' *Colloids Surf. A Physicochem. Eng.*, **443** 525–534 (2014)
38. Yang, J, Li, H, Yi, Z, Liao, M, Qin, Z, ''Stable Superhydrophobic Wood Surface Constracting by KH580 and Nano-Al_2O_3 on Polydopamine Coating with Two Process Methods.'' *Colloids Surf. A: Physicochem. Eng.*, 128219 (2022)
39. Sow, C, Riedl, B, Blanchet, P, ''UV-waterborne Polyurethane-acrylate Nanocomposite Coatings Containing Alumina and Silica Nanoparticles for Wood: Mechanical, Optical, and Thermal Properties Assessment.'' *J. Coat. Technol. Res.*, **8** (2) 211–221 (2011)
40. Nkeuwa, WN, Riedl, B, Landry, V, ''Transparent UV-cured Clay/UV-based Nanocomposite Coatings on Wood Substrates: Surface Roughness and Effect of Relative Humidity on Optical Properties.'' *J. Coat. Technol. Res.*, **14** (3) 555–569 (2017)
41. Pique, TM, Perez, CJ, Alvarez, VA, Vazquez, A, ''Water Soluble Nanocomposite Films Based on Poly (vinyl alcohol) and Chemically Modified Montmorillonites.'' *J. Compos. Mater.*, **48** (5) 545–553 (2014)
42. Xu, X, Liu, F, Jiang, L, Zhu, J, Haagenson, D, Wiesenborn, DP, ''Cellulose Nanocrystals vs. Cellulose Nanofibrils: A Comparative Study on Their Microstructures and Effects as Polymer Reinforcing Agents.'' *ACS Appl. Mater. Interfaces*, **5** (8) 2999–3009 (2013)
43. Calovi, M, Rossi, S, ''Impact of High Concentrations of Cellulose Fibers on the Morphology, Durability and Protective Properties of Wood Paint.'' *Coatings*, **13** (4) 721 (2023)
44. Zou, H, Wu, S, Shen, J, ''Polymer/Silica Nanocomposites: Preparation, Characterization, Properties, and Applications.'' *Chem. Rev.*, **108** (9) 3893–3957 (2008)
45. Duan, X, Liu, S, Huang, E, Shen, X, Wang, Z, Li, S, Jin, C, ''Superhydrophobic and Antibacterial Wood Enabled by Polydopamine-Assisted Decoration of Copper Nanoparticles.'' *Colloids Surf. A Physicochem. Eng.*, **602** 125145 (2020)
46. Qian, L, Long, L, Xu, JF, ''Surface Modification of Nanotitanium and its Effect on the Antibacterial Property of Waterborne Wood Coating.'' *Key Eng. Mater.*, **609** 88–93 (2014)
47. Cheng, L, Ren, S, Lu, X, ''Application of Eco-friendly Waterborne Polyurethane Composite Coating Incorporated with Nano Cellulose Crystalline and Silver Nano Particles on Wood Antibacterial Board.'' *Polymers*, **12** (2) 407 (2020)
48. Calovi, M, Coroneo, V, Palanti, S, Rossi, S, ''Colloidal Silver as Innovative Multifunctional Pigment: The Effect of Ag Concentration on the Durability and Biocidal Activity of Wood Paints.'' *Prog. Org. Coat.*, **175** 107354 (2023)
49. Gaylarde, C, Morton, L, Loh, K, Shirakawa, M, ''Biodeterioration of External Architectural Paint Films–A Review.'' *Int. Biodeterior. Biodegrad.*, **65** (8) 1189–1198 (2011)
50. Wiemann, MC, ''Characteristics and Availability of Commercially Important Woods.'' *Forest Products Laboratory. Wood Handbook: Wood as an engineering material. Madison: United States Department of Agriculture: Forest Service*, 2010
51. Yan, X, Chang, Y, Qian, X, ''Effect of the Concentration of Pigment Slurry on the Film Performances of Waterborne Wood Coatings.'' *Coatings*, **9** (10) 635 (2019)
52. Yan, X, Wang, L, Qian, X, ''Influence of Thermochromic Pigment Powder on Properties of Waterborne Primer Film for Chinese Fir.'' *Coatings*, **9** (11) 742 (2019)
53. Reinprecht, L, Panek, M, ''Effect of Pigments in Paints on the Natural and Accelerated Ageing of Spruce Wood Surfaces.'' *Acta Fac. Xylologiae*, **55** (1) 71–84 (2013)
54. Kaestner, D, Petutschnigg, A, Schnabel, T, Illy, A, Taylor, A, ''Influence of Wood Surface Color on the Performance of Luminescent Pigments.'' *For. Prod. J.*, **66** (3–4) 211–213 (2016)
55. Liu, Y, Yu, Z, Zhang, Y, Wang, H, ''Microbial Dyeing for Inoculation and Pigment Used in Wood Processing: Opportunities and Challenges.'' *Dyes Pigm.*, **186** 109021 (2021)
56. Vega Gutierrez, SM, Stone, DW, He, R, Vega Gutierrez, PT, Walsh, ZM, Robinson, SC, ''Potential Use of the

Pigments from Scytalidium cuboideum and Chlorociboria aeruginosa to Prevent 'Greying' Decking and Other Outdoor Wood Products.'' *Coatings*, **11** (5) 511 (2021)
57. Reinprecht, L, Pánek, M, ''Effects of Wood Roughness, Light Pigments, and Water Repellent on the Color Stability of Painted Spruce Subjected to Natural and Accelerated Weathering.'' *BioResources*, **10** (4) 7203–7219 (2015)
58. Zhang, Z-M, Du, H, Wang, W-H, Wang, Q-W, ''Property Changes of Wood-fiber/HDPE Composites Colored by Iron Oxide Pigments After Accelerated UV Weathering.'' *J. For. Res.*, **21** (1) 59–62 (2010)
59. Seretis, G, Manolakos, D, Provatidis, C, ''On the Stainless Steel Flakes Reinforcement of Polymer Matrix Particulate Composites.'' *Compos. B Eng.*, **162** 80–88 (2019)
60. Li, S, Yang, J, Zhao, H, Cai, X, Yang, B, Lu, Y, ''The Role of Stainless Steel Flakes Epoxy Intermediate Nano-coating in the Heavy-duty Nano Organic Coating System.'' *Proc. IOP Conference Series: Materials Science and Engineering*, 2018
61. Qi, C, Dam-Johansen, K, Weinell, CE, Bi, H, Wu, H, ''Enhanced Anticorrosion Performance of Zinc Rich Epoxy Coatings Modified with Stainless Steel Flakes.'' *Prog. Org. Coat.*, **163** 106616 (2022)
62. Russo, F, Fontanari, V, Rustighi, E, Lekka, M, Hernandez, L, Rossi, S, ''Composite Vitreous Enamel Coatings with the Addition of 316L Stainless Steel Flakes: Novel Insights on Their Behaviour Under Mechanical Stresses.'' *Surf. Coat. Technol.*, **459** 129393 (2023)
63. Russo, F, Fontanari, V, Rossi, S, ''Abrasion Behavior and Functional Properties of Composite Vitreous Enamel Coatings Fabricated with the Addition of 316L Stainless Steel Flakes.'' *Ceram. Int.*, **48** (16) 23666–23677 (2022)
64. James, J, Lewis, W, Wilshire, B, ''Control of Reflective Properties of Flake Metal Products.'' *Powder Metall.*, **36** (1) 42–46 (1993)
65. Faulkner, EB, Schwartz, RJ, *High Performance Pigments*. Wiley, Hoboken, USA (2009)
66. Maile, FJ, Pfaff, G, Reynders, P, ''Effect Pigments—Past, Present and Future.'' *Prog. Org. Coat.*, **54** (3) 150–163 (2005)
67. Pfaff, G, Bartelt, MR, Maile, FJ, ''Metal Effect Pigments.'' *Phys. Sci. Rev.*, **6** (6) 179–197 (2021)
68. Boidot, A, Gheno, F, Bentiss, F, Jama, C, Vogt, JB, ''Effect of Aluminum Flakes on Corrosion Protection Behavior of Water-Based Hybrid Zinc-Rich Coatings for Carbon Steel Substrate in NaCl Environment.'' *Coatings*, **12** (10) 1390 (2022)
69. Sung, LP, Nadal, ME, McKnight, ME, Marx, E, Laurenti, B, ''Optical Reflectance of Metallic Coatings: Effect of Aluminum Flake Orientation.'' *J. Coat. Technol.*, **74** 55–63 (2002)
70. Kiehl, A, Greiwe, K, ''Encapsulated Aluminium Pigments.'' *Prog. Org. Coat.*, **37** (3–4) 179–183 (1999)
71. ASTM G154:16, ''Standard Practice for Operating Fluorescent Ultraviolet (UV) Lamp Apparatus for Exposure ofNonmetallic Materials.'' *West Conshohocken (PA): ASTM International*, 1-10 (2016)
72. UNI 9429:2022, ''Finiture del legno e dei mobili - Determinazione della resistenza delle superfici agli sbalzi di temperatura.'' *UNI - Ente Nazionale Italiano di Unificazione*, 1-11 (2022)
73. ASTM D3359-17, ''Standard Test Methods for Rating Adhesion by Tape Test.'' *West Conshohocken (PA): ASTM International*, 1-10 (2017)
74. GB/T1733-93, ''Determination of Resistance to Water of Films.'' *Standardization Administration of the People's Republic of China: Beijing*, 1-11 (1993)
75. EN927-5, ''Paints and Varnishes - Coating Materials and Coating Systems for Exterior Wood - Part 5: Assessment of the Liquid Water Permeability.'' *European Standard*, 1-18 (2005)
76. ISO 2815:2000, ''Determinazione Della Durezza Con il mEtodo di Penetrazione Buchholz.'' *UNI - Ente Nazionale Italiano di Unificazione*, 1-10 (2000)
77. ''ISO 11998:2006 - Paints and Varnishes: Determination of Wet-Scrub Resistance and Cleanability of Coatings.'' *BSI British Standards: London, UK*, 1-11 (2006)
78. Rossi, S, Calovi, M, Dalpiaz, D, Fedel, M, ''The Influence of NIR Pigments on Coil Coatings' Thermal Behaviors.'' *Coatings*, **10** (6) 514 (2020)
79. Rosati, A, Fedel, M, Rossi, S, ''Laboratory Scale Characterization of Cool Roof Paints: Comparison Among Different Artificial Radiation Sources.'' *Prog. Org. Coat.*, **161** 106464 (2021)
80. Calovi, M, Rossi, S, ''From Wood Waste to Wood Protection: New Application of Black Bio Renewable Water-Based Dispersions as Pigment for Bio-based Wood Paint.'' *Prog. Org. Coat.*, **180** 107577 (2023)
81. Calovi, M, Rossi, S, Deflorian, F, Dirè, S, Ceccato, R, Guo, X, Frankel, GS, ''Effects of Graphene-Based Fillers on Cathodic Delamination and Abrasion Resistance of Cataphoretic Organic Coatings.'' *Coatings*, **10** (6) 602 (2020)
82. Calovi, M, Rossi, S, Deflorian, F, Dirè, S, Ceccato, R, ''Graphene-based Reinforcing Filler for Double-Layer Acrylic Coatings.'' *Materials*, **13** (20) 4499 (2020)
83. ASTM-E308-18, ''Standard Practice for Computing the Colors of Objectives by Using the CIE System.'' *West Conshohocken (PA): ASTM International*, 1-45 (2018)
84. Mokrzycki, W, Tatol, M, ''Colour Difference ΔE-A Survey.'' *Mach. Graph. Vis.*, **20** (4) 383–411 (2011)
85. Calovi, M, Russo, F, Rossi, S, ''Esthetic Performance of Thermochromic Pigments in Cataphoretic and Sprayed Coatings for Outdoor Applications.'' *J. Appl. Polym. Sci.*, **138** (26) 50622 (2021)
86. Fengel, D, Wegener, G, *Wood: Chemistry, Ultrastructure, Reactions*. Walter de Gruyter, Berlin (2011)
87. Ghavidel, A, Hosseinpourpia, R, Gelbrich, J, Bak, M, Sandu, I, ''Microstructural and Chemical Characteristics of Archaeological White Elm (Ulmus laevis P.) and Poplar (Populus spp.).'' *Appl. Sci.*, **11** (21) 10271 (2021)
88. Ghavidel, A, Bak, M, Hofmann, T, Vasilache, V, Sandu, I, ''Evaluation of Some Wood-Water Relations and Chemometric Characteristics of Recent Oak and Archaeological Oak Wood (*Quercus robur*) with Archaeometric Value.'' *J. Cult. Herit.*, **51** 21–28 (2021)
89. Gu, Y, Bian, H, Wei, L, Wang, R, ''Enhancement of Hydrotropic Fractionation of Poplar Wood Using Autohydrolysis and Disk Refining Pretreatment: Morphology and Overall Chemical Characterization.'' *Polymers*, **11** (4) 685 (2019)
90. Bian, H, Li, G, Jiao, L, Yu, Z, Dai, H, ''Enzyme-assisted Mechanical Fibrillation of Bleached Spruce Kraft Pulp for Producing Well-dispersed and Uniform-Sized Cellulose Nanofibrils.'' *Bioresources*, **11** (4) 10483–10496 (2016)
91. Chiantore, O, Trossarelli, L, Lazzari, M, ''Photooxidative Degradation of Acrylic and Methacrylic Polymers.'' *Polymer*, **41** (5) 1657–1668 (2000)
92. Calovi, M, Rossi, S, ''Durability of Acrylic Cataphoretic Coatings Additivated with Colloidal Silver.'' *Coatings*, **12** (4) 486 (2022)

93. Kaczmarek, H, Kamińska, A, van Herk, A, ''Photooxidative Degradation of Poly(alkyl methacrylate)s.'' *Eur. Polym. J.*, **36** (4) 767–777 (2000)
94. Luo, H, Li, X, Dong, C, Xiao, K, Cheng, X, ''Influence of uv Light on Passive Behavior of the 304 Stainless Steel in Acid Solution.'' *J. Phys. Chem. Solids*, **74** (5) 691–697 (2013)
95. Li, H, Osman, H, Kang, C, Ba, T, ''Numerical and Experimental Investigation of UV Disinfection for Water Treatment.'' *Appl. Therm. Eng.*, **111** 280–291 (2017)
96. Heidarinejad, G, Bozorgmehr, N, Safarzadeh, M, ''Effect of Highly Reflective Material on the Performance of Water Ultraviolet Disinfection Reactor.'' *J. Water Process. Eng.*, **36** 101375 (2020)
97. Yan, X, Qian, X, Chang, Y, Lu, R, Miyakoshi, T, ''The Effect of Glass Fiber Powder on the Properties of Waterborne Coatings with Thermochromic Ink on a Chinese Fir Surface.'' *Polymers*, **11** (11) 1733 (2019)
98. GB/T11186.3-90, ''Method of Measurement of Coating Color. Part III: Calculation of Chromatic Aberration.'' *Standardization Administration of the People's Republic of China: Beijing*, 1-12 (1990)
99. Calovi, M, Rossi, S, ''Olive Pit Powder as Multifunctional Pigment for Waterborne Paint: Influence of the Bio-based Filler on the Aesthetics, Durability and Mechanical Features of the Polymer Matrix.'' *Ind. Crops Prod.*, **194** 116326 (2023)
100. Seretis, GV, Polyzou, AK, Manolakos, DE, Provatidis, CG, ''Effect of Stainless Steel Flakes Content on Mechanical Properties and Microstructure of Cast 96.66% Pure Aluminum.'' *Proc. Nano Hybrids and Composites*, 2018
101. Calovi, M, Rossi, S, ''Durability and Thermal Behavior of Functional Paints Formulated with Recycled-Glass Hollow Microspheres of Different Size.'' *Materials*, **16** (7) 2678 (2023)
102. Bishara, A, Kramberger-Kaplan, H, Ptatschek, V, ''Influence of Different Pigments on the Facade Surface Temperatures.'' *Energy Procedia*, **132** 447–453 (2017)
103. Zhang, J, Lin, W, Zhu, C, Lv, J, Zhang, W, Feng, J, ''Dark, Infrared Reflective, and Superhydrophobic Coatings by Waterborne Resins.'' *Langmuir*, **34** (19) 5600–5605 (2018)
104. Synnefa, A, Santamouris, M, Apostolakis, K, ''On the Development, Optical Properties and Thermal Performance of Cool Colored Coatings for the Urban Environment.'' *Sol. Energy*, **81** (4) 488–497 (2007)